Novel red-emitting phosphors, $(Mg_{(1-x-y)}Mn_xDy_y)Al_2Si_2O_8$ and $(Mg_{(1-x-y)}Mn_xTm_y)Al_2Si_2O_8$

Esra Öztürk, Nilgun Kalaycioglu Ozpozan & Serkan Dayan

Journal of Thermal Analysis and Calorimetry
An International Forum for Thermal Studies

ISSN 1388-6150
Volume 117
Number 2

J Therm Anal Calorim (2014)
117:573-578
DOI 10.1007/s10973-014-3791-6

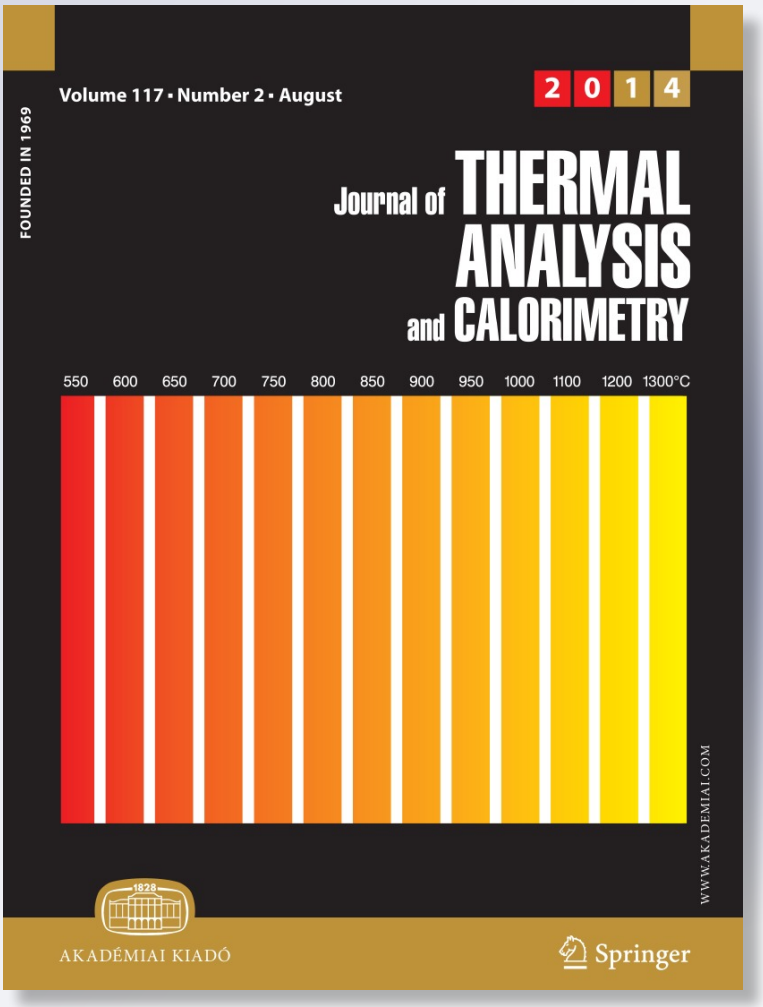

Springer

Your article is protected by copyright and all rights are held exclusively by Akadémiai Kiadó, Budapest, Hungary. This e-offprint is for personal use only and shall not be self-archived in electronic repositories. If you wish to self-archive your article, please use the accepted manuscript version for posting on your own website. You may further deposit the accepted manuscript version in any repository, provided it is only made publicly available 12 months after official publication or later and provided acknowledgement is given to the original source of publication and a link is inserted to the published article on Springer's website. The link must be accompanied by the following text: "The final publication is available at link.springer.com".



Author's personal copy

J Therm Anal Calorim (2014) 117:573–578
DOI 10.1007/s10973-014-3791-6

Novel red-emitting phosphors, $(Mg_{(1-x-y)}Mn_xDy_y)Al_2Si_2O_8$ and $(Mg_{(1-x-y)}Mn_xTm_y)Al_2Si_2O_8$

Esra Öztürk · Nilgun Kalaycioglu Ozpozan · Serkan Dayan

Received: 23 August 2013 / Accepted: 23 March 2014 / Published online: 13 April 2014
© Akadémiai Kiadó, Budapest, Hungary 2014

Abstract Mn^{4+} doped and Dy^{3+}, Tm^{3+} co-doped $MgAl_2Si_2O_8$-based phosphors were prepared by conventional solid state reaction at 1,300 °C. They were characterized by thermogravimetry, differential thermal analysis, X-ray powder diffraction, photoluminescence, and scanning electron microscopy. The luminescence mechanism of the phosphors, which showed broad red emission bands in the range of 600–715 nm and had a different maximum intensity when activated by UV illumination, was discussed. Such a red emission can be attributed to the $^2E \rightarrow {}^4A_2$ transitions of Mn^{4+}.

Keywords Inorganic compounds · Luminescence · Thermogravimetry (TG) · X-ray diffraction · Electron microscopy

Introduction

Luminescent materials with long afterglow are kinds of energy storage materials that can absorb both UV and visible light from the sun and gradually release this energy in the dark at a certain wavelength. These kinds of long lasting phosphors have been widely studied by many researchers [1–3].

E. Öztürk (✉)
Department of Materials Science and Engineering, Faculty of Engineering, Karamanoğlu Mehmetbey University, Karaman 70200, Turkey
e-mail: esracircir@gmail.com

N. K. Ozpozan · S. Dayan
Department of Chemistry, Faculty of Science, Erciyes University, Kayseri 38039, Turkey

Silicates, therefore, are suitable hosts for phosphors because of their high physical and chemical stability. The luminescence of rare-earth ions in the silicate host has been studied for a long time. In recent years, silicate phosphors have been reported by researchers [4–13].

In this paper, $MgAl_2Si_2O_8:Mn^{4+},Dy^{3+}$ and $MgAl_2Si_2O_8:Mn^{4+},Tm^{3+}$-based phosphors were synthesized by solid state reaction at 1,300 °C. Their thermal behavior, crystal structure, morphological characterization, photoluminescence properties, and excitation mechanism were then investigated.

Experimental

$MgAl_2Si_2O_8:Mn^{4+},Dy^{3+}$ and $MgAl_2Si_2O_8:Mn^{4+},Tm^{3+}$ phosphors were synthesized using the solid state technique. Starting materials: $4MgCO_3Mg(OH)_25H_2O$ (A.R.) in triclinic crystal system with lattice parameters $a = 826.16$ pm, $b = 1164.27$ pm, $c = 1742.91$ pm; $\alpha = 144.93°$, $\beta = 47.83°$, $\gamma = 132.09°$, and $V = 684.85 \times 10^6$ pm^3, Al_2O_3 (99.0 %) compatible with JCPDS file number 75-1864, SiO_2 (99.8 %) compatible with JCPDS file number 78-1422, MnO_2 (99.0 %) in tetragonal crystal system with lattice parameters $a = 439.57$ pm, $c = 287.30$ pm, and V = 55.51 $\times 10^6$ pm^3, Dy_2O_3 (99.99 %) compatible with JCPDS file number 09-0197 and Tm_2O_3 (99.90 %) compatible with JCPDS file number 02-0631 were weighed according to the nominal compositions of $(Mg_{0.88}Mn_{0.10}Dy_{0.02})Al_2Si_2O_8$ and $(Mg_{0.88}Mn_{0.10}Tm_{0.02})$-$Al_2Si_2O_8$. These powders were mixed homogeneously in an agate mortar for 3 h. Small quantities of H_3BO_3 were added as a flux during the mixing. Its crystal system is triclinic with lattice parameters $a = 492.50$ pm, $b = 1020.50$ pm, $c = 989.82$ pm; $\alpha = 140.51°$, $\beta = 94.55°$, $\gamma = 71.09°$, and $V = 287.00 \times 10^6$ pm^3. A small amount of each sample was taken for

Author's personal copy

thermal analysis (DTA/TG) to study the phase-forming process. Thermogravimetry (TG) and differential thermal analysis (DTA) were carried out by using a DTA/TG system (Perkin Elmer Diamond type). The samples were heated at a rate of 10 °C min^{-1} from room temperature to 1,300 °C, in the nitrogen atmosphere.

Afterward, the sintering conditions of the phosphors, including the pre-firing temperature and synthesizing temperature, were determined in two steps: first, the mixtures were pre-fired at 900 °C for 3 h in a porcelain crucible in air, and then the pre-fired samples were sintered at 1,300 °C for 3 h in an air atmosphere, in a porcelain crucible. After these procedures, the phosphors were obtained and their crystal structures were examined by X-ray diffraction (XRD) analysis using a Bruker AXS D8 Advance diffractometer which was run at 20–60 kV and 6–80 mA, $2\theta = 10°–90°$ and a step of 0.002° using CuKα X-ray.

Scanning electron microscopy (SEM) images and EDX analysis were performed on a LEO 440 model scanning electron microscope using an accelerating voltage of 20 kV.

The decay time, excitation, and emission spectra of the phosphors were recorded by a Perkin Elmer LS 45 model luminescence spectrophotometer with xenon lamp.

Results and discussion

Thermal behavior, crystallization, and morphology

Figure 1 illustrates the DTA/TG curves of starting materials for $MgAl_2Si_2O_8$: Mn^{4+},Dy^{3+}. The curves below 200 °C include the dehydration of $4MgCO_3{\cdot}Mg(OH)_2{\cdot}5H_2O$ and the decomposition of H_3BO_3 which changes into B_2O_3. The first endothermic peak is (at 240 °C, point A) attributed to the deviation of the hydroxyl group from $Mg(OH)_2$. The second endothermic peak shows (at 437 °C, point B) the decomposition of $MgCO_3$ which changes into MgO.

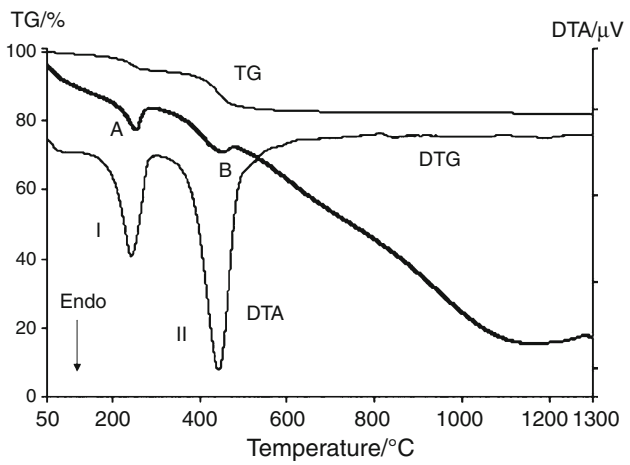

Fig. 1 TG/DTA/DTG curves of $MgAl_2Si_2O_8$:Mn^{4+},Dy^{3+} phosphor

From the above DTA/TG analysis, we carried out the sintering of the phosphors in two steps: first, the samples were pre-fired at 900 °C for 3 h to achieve the dehydration and decomposition of H_3BO_3, $MgCO_3$, and $Mg(OH)_2$, and to help the doped Mn^{4+} and rare-earth ions to substitute; next the phosphors were prepared at 1,300 °C for 3 h in air. Actually, the crystal systems were not observed at 900 °C, but at 1,300 °C for 3 h the $(Mg_{1-x-y}Mn_xDy_y)Al_2Si_2O_8$ and $(Mg_{1-x-y}Mn_xTm_y)Al_2Si_2O_8$ ($x = 0.10$ and $y = 0.02$) non-stoichiometric triclinic crystal systems are observed (Fig. 2).

The XRD patterns of phosphors obtained at 900 °C and 1,300 °C for 3 h in air are shown in Fig. 2a, b. The unit cell parameters of phosphor crystallized in the triclinic system are listed in Table 1.

Figures 3 and 4 show the images and EDX analysis obtained from the scanning electron microscopy (SEM) of the phosphors calcined at 1,300 °C for 3 h by using solid state reactions. The microstructures of the phosphor consisted of regular fine grains with an average size of about 0.6–2.5 μm.

Photoluminescence properties

Figure 5 shows the excitation and emission spectra of the $MgAl_2Si_2O_8$:Mn^{4+},Dy^{3+} phosphor annealed at 1,300 °C. The excitation spectrum of the $MgAl_2Si_2O_8$:Mn^{4+},Dy^{3+} phosphor observed with Mn^{4+} emission at 674 nm ($^2E \rightarrow {}^4A_2$ transitions) consists of an excitation band with a maximum at 257 nm. Under 257 nm UV excitation, the $MgAl_2Si_2O_8$:Mn^{4+},Dy^{3+} phosphor shows a strong red luminescence ranging from 600 to 750 nm with a maximum, at 674 nm and some lines (588, 656, and 722 nm) in the longer wavelength region. The red emission at 674 nm, which can be viewed as a typical Mn^{4+} emission, was ascribed to $^2E \rightarrow {}^4A_2$ transitions [14]. The emission bands at 588 and 656 nm are due to the transitions of Dy^{3+} $^5F_{9/2} \rightarrow {}^6H_{13/2}$ ve $^5F_{9/2} \rightarrow {}^6H_{11/2}$, respectively [15, 16]. In order to identify the origin of the emission band of the $MgAl_2Si_2O_8$:Mn^{4+},Dy^{3+} phosphor at 722 nm, we took into account the emission spectrum of the undoped $MgAl_2Si_2O_8$ sample under the same excitation conditions. We reported the spectrum of the undoped $MgAl_2Si_2O_8$ in our previous article [17]. It showed an emission ranging from 600 to 800 nm with the three maximum at 617, 710, and 720 nm. The broad $MgAl_2Si_2O_8$ emission band can be attributed to the recombination of an electron on a donor with a hole on an acceptor. The recombination was caused by crystal defects which occurred in the undoped $MgAl_2Si_2O_8$ during the solid state process. The emission band

Author's personal copy

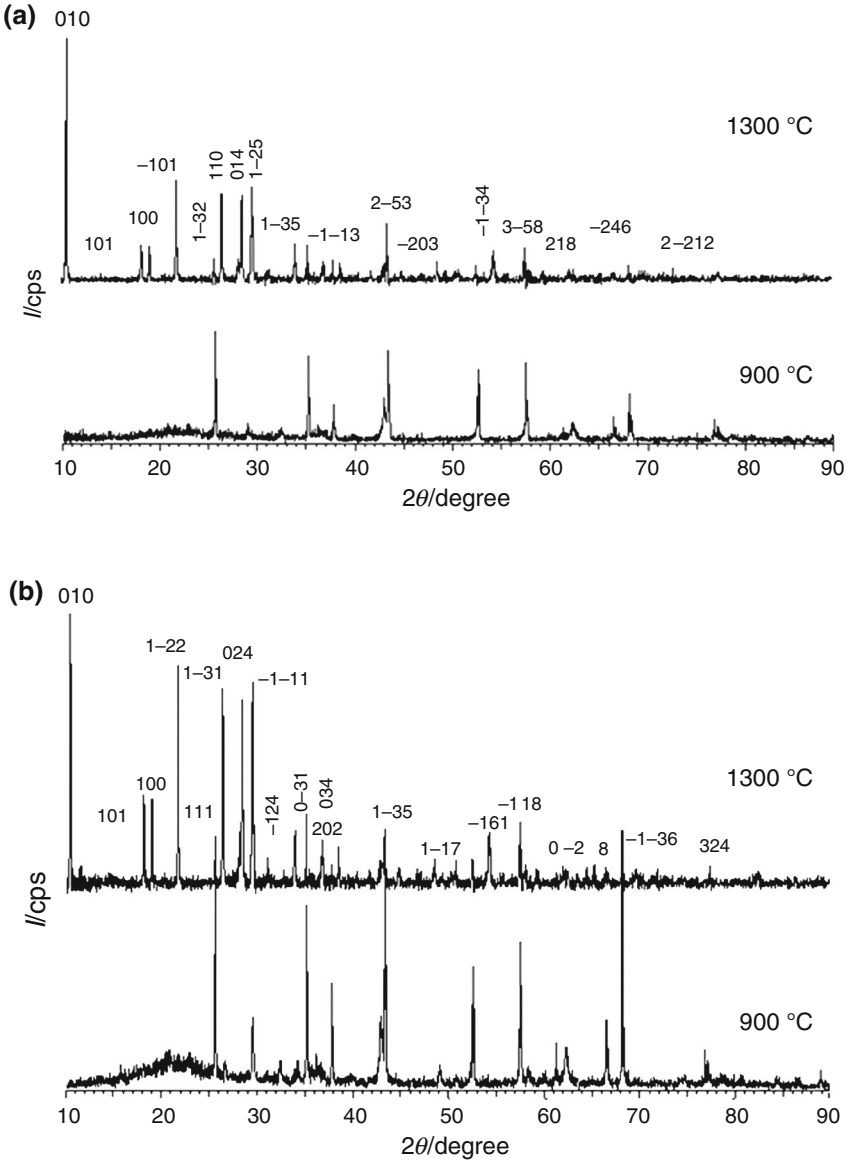

Fig. 2 XRD patterns of phosphors, **a** $(Mg_{0.88}Mn_{0.10}Dy_{0.02})Al_2Si_2O_8$, **b** $(Mg_{0.88}Mn_{0.10}Tm_{0.02})Al_2Si_2O_8$

Table 1 Unit cell parameters of phosphors

Phosphor	*a*/pm	*b*/pm	*c*/pm	$V/\times 10^6$ pm^3	*α*/°	*β*/°	*γ*/°
$(Mg_{0.88}Mn_{0.10}Dy_{0.02})Al_2Si_2O_8$	605.04	1048.57	1565.72	716.62	109.68	64.99	126.75
$(Mg_{0.88}Mn_{0.10}Tm_{0.02})Al_2Si_2O_8$	802.34	1044.07	1371.35	579.49	47.46	44.15	54.57

at 722 nm in the $MgAl_2Si_2O_8:Mn^{4+},Dy^{3+}$ phosphor has the same profile as that of the undoped $MgAl_2Si_2O_8$; thus, it can be ascribed to the host emission.

The excitation and emission spectra of the $MgAl_2Si_2O_8:Mn^{4+},Tm^{3+}$ phosphor are shown in Fig. 6. Under excitation at 256 nm, the $MgAl_2Si_2O_8:Mn^{4+},Tm^{3+}$ phosphor exhibits a strong red luminescence. The excitation spectrum of the $MgAl_2Si_2O_8:Mn^{4+},Tm^{3+}$ phosphor observed with Mn^{4+} emission at 673 nm ($^2E \rightarrow {}^4A_2$ transitions) shows a strong excitation band with maximum at 256 nm. When the phosphor was excited at 256 nm, only one emission peak located around 673 nm was observed on the emission spectrum. Such a broad red emission at 673 nm can be viewed as the typical emission of $^2E \rightarrow {}^4A_2$

Author's personal copy

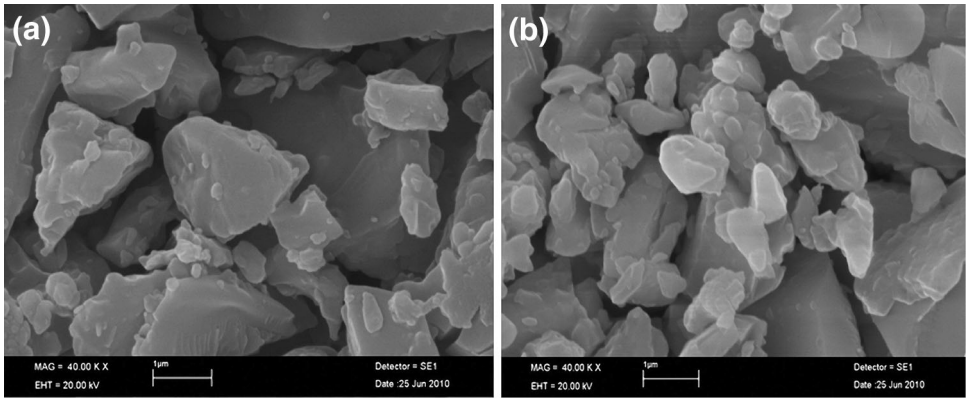

Fig. 3 SEM image of **a** $(Mg_{0.88}Mn_{0.10}Dy_{0.02})Al_2Si_2O_8$ phosphor, **b** $(Mg_{0.88}Mn_{0.10}Tm_{0.02})Al_2Si_2O_8$ phosphor

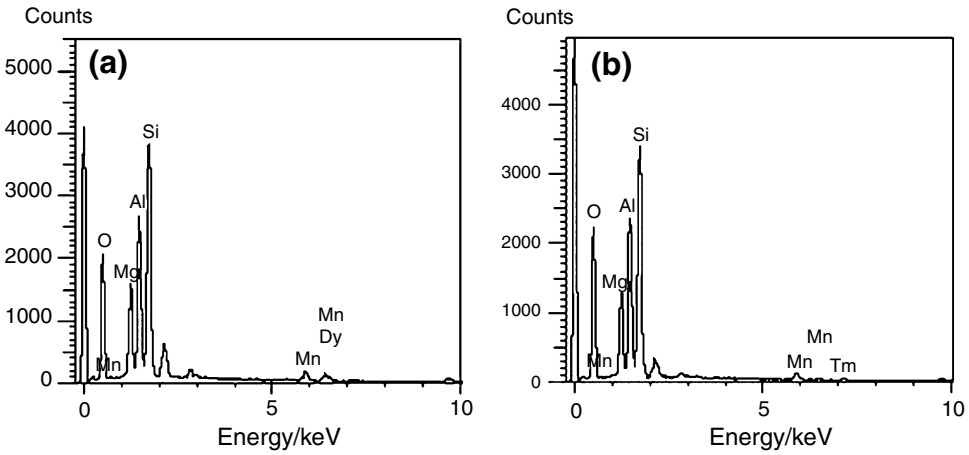

Fig. 4 EDX analysis of **a** $(Mg_{0.88}Mn_{0.10}Dy_{0.02})Al_2Si_2O_8$ phosphor, **b** $(Mg_{0.88}Mn_{0.10}Tm_{0.02})Al_2Si_2O_8$ phosphor

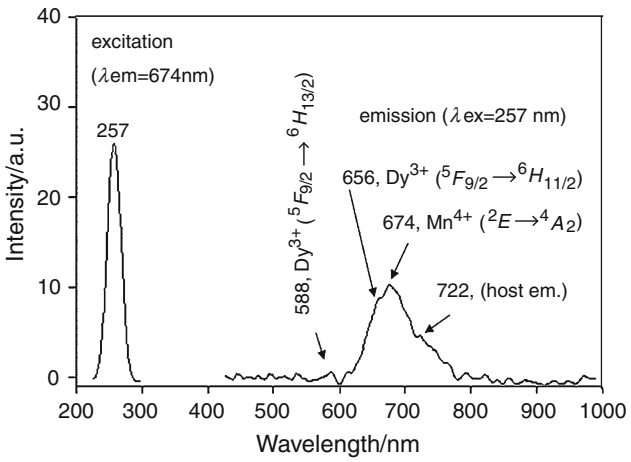

Fig. 5 The excitation and emission spectra of $(Mg_{0.88}Mn_{0.10}Dy_{0.02})$-$Al_2Si_2O_8$ phosphor

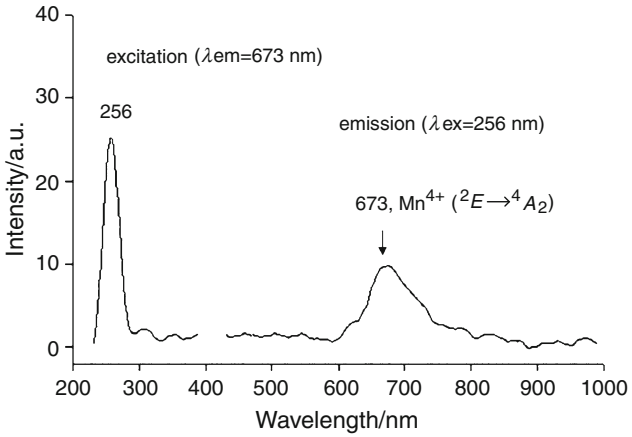

Fig. 6 The excitation and emission spectra of $(Mg_{0.88}Mn_{0.10}Tm_{0.02})$-$Al_2Si_2O_8$ phosphor

transitions of Mn^{4+}. Typical emission peaks of Tm^{3+} were not observed in the emission spectrum of the $MgAl_2Si_2O_8$:Mn^{4+},Tm^{3+} phosphor.

When considering the excitation mechanism, in Figs. 5 and 6, there is only one possible explanation for the excitation bands of the $MgAl_2Si_2O_8$:Mn^{4+},Dy^{3+} and $MgAl_2Si_2O_8$:Mn^{4+},Tm^{3+}

Author's personal copy

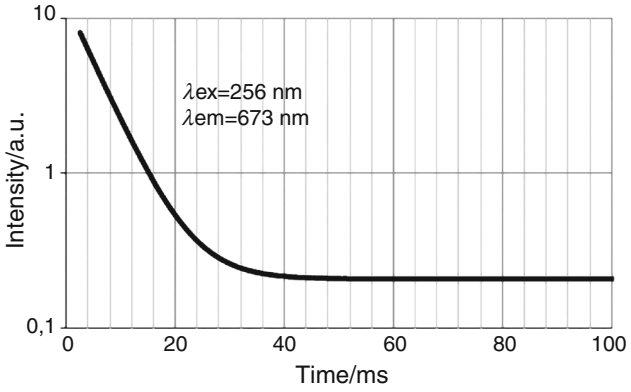

Fig. 7 The decay curves of the $(Mg_{0.88}Mn_{0.10}Tm_{0.02})Al_2Si_2O_8$ phosphors

phosphors: this is host crystal absorption. The excitation spectra of the host $MgAl_2Si_2O_8$ [17] are in agreement with the excitation spectra of the $MgAl_2Si_2O_8$:Mn^{4+},Dy^{3+} (Fig. 5) and $MgAl_2Si_2O_8$:Mn^{4+},Tm^{3+} (Fig. 6) phosphors. This indicates that all of the excitation band of the $MgAl_2Si_2O_8$:Mn^{4+},Dy^{3+} and $MgAl_2Si_2O_8$:Mn^{4+},Tm^{3+} phosphors at 256 and 257 nm arise from host lattice absorption. The excitation energy at 256 nm and 257 nm is first captured and then transferred to the Mn^{4+} and Dy^{3+} ions by the host crystal. The presence of the $MgAl_2Si_2O_8$ host crystal's excitation band in the excitation spectra of $MgAl_2Si_2O_8$:Mn^{4+},Dy^{3+} and $MgAl_2Si_2O_8$:Mn^{4+}, Tm^{3+} phosphors shows that an energy transfer takes place from the $MgAl_2Si_2O_8$ host crystal to the Mn^{4+} and Dy^{3+} ions. The excitation energy of the host crystal $MgAl_2Si_2O_8$ doped with Mn^{4+} and Dy^{3+} ions can be non-radiatively transferred to Mn^{4+} and Dy^{3+} ions. As shown in Fig. 6, the energy transfer from the $MgAl_2Si_2O_8$ to Mn^{4+} ions is complete. However, Fig. 5 shows that the emission band at 722 nm from the $MgAl_2Si_2O_8$ host lattice can still be observed in the emission spectrum $MgAl_2Si_2O_8$:Mn^{4+},Dy^{3+}. Therefore, the energy transfer from the $MgAl_2Si_2O_8$ host crystal to the Mn^{4+} and Dy^{3+} ions is not complete. In addition, there is no energy transfer from the host crystal $MgAl_2Si_2O_8$ to the Tm^{3+} ions.

The luminescence decay curve of the $MgAl_2Si_2O_8$:Mn^{4+},Tm^{3+} phosphor is shown in Fig. 7. Decay time can be calculated by a curve fitting method based on the following single exponential equation:

$$I = A_1\exp(-t/\tau_1) + C,$$

where I is phosphorescence intensity, A_1, C are constants, t is time; and τ_1 is the lifetime for the exponential components. Decay time (τ_1) for exponential component of $MgAl_2Si_2O_8$:Mn^{4+},Tm^{3+} phosphor was 5.477 ms. The $MgAl_2Si_2O_8$:Mn^{4+},Tm^{3+} phosphor shows much longer afterglow than the undoped $MgAl_2Si_2O_8$ phosphor which indicates that Mn^{4+} and Tm^{3+} ions play an important role in prolonging the afterglow.

The decay time of the $MgAl_2Si_2O_8$:Mn^{4+}, Dy^{3+} phosphor cannot be detected and calculated in the same conditions.

Conclusions

In this report, $(Mg_{0.88}Mn_{0.10}Dy_{0.02})Al_2Si_2O_8$ and $(Mg_{0.88}Mn_{0.10}Tm_{0.02})Al_2Si_2O_8$ red phosphors were first prepared by using the solid state reaction at 1,300 °C for 3 h. The phosphors had a triclinic crystal system. Under UV excitation at 256 nm and 257 nm, $MgAl_2Si_2O_8$:Mn^{4+},Dy^{3+} and $MgAl_2Si_2O_8$:Mn^{4+},Tm^{3+} phosphors showed strong red luminescence. The mechanism of excitation in $MgAl_2Si_2O_8$-based phosphors was explained by an energy transfer from the $MgAl_2Si_2O_8$ host crystal to the Mn^{4+} and Dy^{3+} ions.

Acknowledgements This work was supported by Erciyes University EUBAP under project number FBD-09-804.

References

1. Lin Y, Tang Z, Zhang Z, Nan C. Luminescence of Eu^{2+} and Dy^{3+} activated $R_3MgSi_2O_8$-based (R = Ca, Sr, Ba) phosphors. J Alloys Compd. 2003;348:76–9.
2. Wang Y, Wang Z, Zhang P, Hong Z, Fan X, Qian G. Preparationof Eu^{2+} and Dy^{3+} co-activated $CaAl_2Si_2O_8$-based phosphor and its optical properties. Mater Lett. 2004;5:3308–11.
3. Chang CK, Mao DL. Long lasting phosphorescence of Sr Al O:Eu, Dy thin films by magnetron sputtering. Thin Solid Films. 2004;460:48–52.
4. Blasse G, Wanmaker WL, Ter Vrugt JW, Bril A. Philips Res Rep. 1968;23:189.
5. Barry TL. Equilibria and Eu^{2+} luminescence of subsolidus phases bounded by $Ba_3MgSi_2O_8$, $Sr_3MgSi_2O_8$ and $Ca_3MgSi_2O_8$. J Electrochem Soc. 1968;115:733–8.
6. Barry TL. Fluorescence of Eu^{2+}-activated phases in binary alkaline earth orthosilicate systems. J Electrochem Soc. 1968;115:1181–4.
7. Moore PB, Araki T. Atomic arrangement of merwinite, $Ca_3Mg[SiO_4]_2$, an unusual dense-packed structure of geophysi cal interest. Am Miner. 1972;57:1355–74.
8. Çırçır E, Kalaycioglu Ozpozan N. Host-sensitized phosphorescence of Mn^{4+}, $Pr^{3+,\ 4+}$ and Nd^{3+} in $MgAl_2Si_2O_8$. Mater Res Bull. 2012;47:1138–41.
9. Çırçır E, Ozpozan Kalaycioglu N. Host-sensitized phosphorescence of Mn^{4+}, Eu^{3+} and Yb^{3+} in $MgAl_2Si_2O_8$. J Therm Anal Calorim. 2012;110:1179–83.
10. Kalaycioglu Ozpozan N, Çırçır E. Red phosphors in $MgAl_2Si_2O_8$ doping with Mn^{4+}, Gd^{3+} and Lu^{3+} and host-sensitized luminescence properties. J Therm Anal Calorim. 2013;111:273–7.
11. Ye S, Liu Z, Wang X, Wang J, Wang L, Jing X. Emission properties of Eu^{2+}, Mn^{2+} in $MAl_2Si_2O_8$ (M = Sr, Ba). J Lumin. 2009;129:50–4.
12. Clabau F, Garcia A, Bonville P, Ganbeau D, Mercier T, Deniard P. Fluorescence and phosphorescence properties of the low temperature forms of the $MAl_2Si_2O_8$:Eu^{2+} (M = Ca, Sr, Ba) compounds. J Solid State Chem. 2008;181:1456–61.

Author's personal copy

13. Ding Y, Zhang Y, Wang Z, Li W, Mao D, Han H. Photoluminescence of Eu single doped and Eu/Dy codoped $Sr_2Al_2SiO_7$ phosphors with long persistence. J Lumin. 2009;129:294–9.
14. Pan XY, Liu GK. Influence of Mg^{2+} on luminescence efficiency and charge compensating mechanism in phosphor $CaAl_{12}O_{19}$:-Mn^{4+}. J Lumin. 2011;131:465–8.
15. Cheng X. Comparison study of the luminescent properties of the white-light long afterglow phosphors: $Ca_xMgSi_2O_{5+x}$:Dy^{3+} ($x = 1, 2, 3$). J Lumin. 2009;129:531–5.
16. Jia W. Crystal growth and characterization of Eu^{2+}, Dy^{3+}:$SrAl_2O_4$ and Eu^{2+}, Nd^{3+}:$CaAl_2O_4$ by the LHPG method. J Cryst Growth. 1999;200:179–84.
17. Ozpozan Kalaycioglu N, Çırçır E. Synthesis and phosphorescence properties of Mn^{4+}, La^{3+} and Ho^{3+} in $MgAl_2Si_2O_8$. J Alloys Compd. 2012;510:6–10.